Stock or Flow? Carbon Payment Designs for Soil Carbon Sequestration *

Khyati Malik

malikk@nber.org

National Bureau of Economic Research

1050 Massachusetts Avenue

Cambridge, MA 02138

August 19, 2026

*Funding from the USDA Postdoctoral Fellowship, New Perspectives on Agricultural Economics, awarded through the National Bureau of Economic Research (NBER), is gratefully acknowledged. I thank James Poterba, Elena Irwin, Sathya Gopalakrishnan, Yongyang Cai, Christopher Knittel, and Gilbert Metcalf for their valuable comments and suggestions. I also thank seminar participants at the 2026 Camp Resources Workshop, 2026 Harvard Environmental Economics Workshop, the 2025 MIT CEEPR Lunch Seminar Series, 2025 NBER Risk and Risk Management in Agricultural Economy Workshop, and the Department of Agricultural and Resource Economics Seminar at North Carolina State University (2025) for helpful feedback.

Abstract

This paper derives closed-form minimum payment conditions for five carbon payment designs aimed at incentivizing soil organic carbon sequestration through conservation tillage, parameterized using EPIC simulations across 70 Midwestern fields. Incremental payment schemes fail structurally: without penalties for carbon release, the minimum payment required to sustain no-till adoption is strictly increasing in the current SOC stock, generating a cycling equilibrium in which farmers alternate between no-till and conventional tillage. Stock-based payments conditional on conservation practice adoption emerge as the optimal design, requiring lowest payment levels, resolving the additionality problem, and maintaining consistent sequestration incentives throughout the carbon accumulation horizon. Lifetime discounted payments under the optimal design remain below the US social cost of carbon for three of the four soil types studied, and spatially targeted payments reduce total program costs by approximately 22% relative to a uniform carbon price. Flat payment schemes result in long breakeven periods, whereas front-loaded schemes can substantially shorten the breakeven horizon. The framework yields conditions that guarantee incentive-compatibility for the latter class of schemes as the payment stream diminishes over time.

Keywords: Carbon payment design, Voluntary carbon markets, Payment for ecosystem services, Soil carbon sequestration, Additionality

1 Introduction

Payment programs that reward agents for incremental environmental improvements face a structural trap: as sequestration approaches its natural ceiling, the per-period reward declines, giving the agent an incentive to abandon the practice, allow stored carbon to revert, and collect incremental payments anew. In agricultural soil carbon markets, this trap is consequential. Land-based sequestration strategies could offset 10 to 15 gigatons of carbon dioxide equivalents per year globally until 2050 (Griscom et al., 2017; Roe et al., 2021), but long-term no-till adoption covers only 38% of US cropland (Horowitz et al., 2010). Three inherent features of soil carbon dynamics compound the design challenge: sequestration is reversible, with reversion releasing stored carbon rapidly (Kim et al., 2008; Ruseva et al., 2020; Sadatshojaei et al., 2021; Sawadgo and Plastina, 2022); soils have finite storage capacity and sequestration rates decline as stocks approach saturation (Chen et al., 2019; West and Six, 2007; Paustian et al., 2016; Stewart et al., 2007); and conservation practices reduce short-run crop yields, creating a wedge between immediate costs and long-run sequestration benefits (Blevins et al., 1977; Ismail et al., 1994). These features interact with two further frictions that make payment design consequential beyond the level of transfers. First, inframarginal participation is pervasive: for instance, Aspelund and Russo (2026) report that three-quarters of United States Department of Agriculture's Conservation Reserve Program participants would have conserved without payment, and any design that ignores counterfactual behavior wastes program resources on non-additional sequestration. Second, distrust in institutions limits enrollment and effectiveness of standard payment for ecosystem services schemes (Jack et al., 2025; Jayachandran et al., 2017). While prior economic analyses have examined reversibility, delayed accumulation, variable sequestration rates, and yield losses (Antle et al., 2003; Murray et al., 2007; Feng et al., 2002; Raj Kunwar et al., 2025), they have not characterized the conditions under which specific payment designs can or cannot generate lasting adoption. The landscape of carbon farming contracts spans result-based, action-based, and hybrid designs (Raina et al., 2024), yet no unified analytical framework

identifies which design sustains sequestration or why others fail, which is the goal of this work.

I develop a theoretical bioeconomic framework in which a forward-looking farmer maximizes expected discounted profits by choosing between no-till and conventional tillage in each period, trading short-run yield losses against long-run carbon payments. I compare five policy designs: payments proportional to total carbon stock (P1); payments proportional to carbon stock conditional on conservation practice adoption (P2); payments and penalties based on incremental changes in carbon stock (P3); incremental payments conditional on adoption without penalties for reversal (P4); and flat adoption payments (P5). I derive closed-form minimum payment conditions under each design and validate them against a stochastic Bellman equation incorporating uncertainty in soil organic carbon (SOC) dynamics, parameterized using EPIC model (Williams et al., 1989; Izaurralde et al., 2006) simulations across 70 fields in five Midwestern watersheds spanning four soil types based on their drainage characteristics, herein referred to as soil hydrology groups. This integration of biophysical simulation with dynamic optimization addresses sequestration reversibility, carbon saturation, and yield tradeoffs jointly within a unified field-level framework, advancing on prior analyses that have typically treated these constraints in isolation. The dynamic optimization framework builds on the capital-theoretic tradition introduced by Burt (1981) and McConnell (1983), who applied dynamic programming and optimal control to soil resource management decisions, and on recent extensions to soil carbon dynamics and environmental services (Berazneva et al., 2019; Lichtenberg, 2024).

The results identify a clear policy hierarchy. Incremental payment designs fail in both variants. Without penalties for carbon release (P4), a fundamental defection problem emerges: as soils approach carbon saturation, the payment rate required to sustain no-till rises without bound, and farmers rationally revert to conventional tillage regardless of prior sequestration. With penalties (P3), the defection incentive is suppressed but replaced by a lock-in problem at saturation, where farmers face continued yield costs while receiving no

additional payments and facing prohibitive reversal costs. Both outcomes reflect the mechanism identified by Gulati and Vercammen (2005, 2006): declining marginal sequestration benefits as stocks approach their ceiling make incremental designs categorically incompatible with sustained adoption. Flat adoption payments (P5) provide no accountability for actual sequestration and are sub-optimal from a social planner's perspective. Stock-based payments conditional on conservation practice adoption (P2) emerge as the optimal design. This structure holds farmers accountable for maintaining a carbon stock, eliminates the additionality problem that arises when farmers with high legacy carbon stocks collect payments without changing practices, and maintains consistent adoption incentives throughout the sequestration horizon. Lifetime discounted payments under P2 remain below the US social cost of carbon ($190 per ton of CO_2 equivalent) (Farah and Clark, 2022) for three of the four soil types studied, indicating net welfare gains. Required payment rates vary substantially with soil type and initial SOC, and spatially targeted payments calibrated to biophysical characteristics reduce total program costs by approximately 22% relative to uniform payment schemes across the five watersheds studied, with direct implications for the design of conservation incentive programs and voluntary carbon markets.

2 Geographic Focus: U.S. Midwest Agriculture and Carbon Sequestration

The U.S. Midwest, often described as the nation's "food bowl," makes a major contribution to national agricultural production because of its nutrient-rich soils, relatively stable climate, ample freshwater resources, and extensive farmland. Westcott (2010) notes that the Midwest contains some of the world's most productive agricultural soils, which support large-scale cultivation of crops such as corn and soybeans. Warm summers, adequate rainfall, and flat terrain also support consistent yields and efficient mechanized farming, which lowers per-unit production costs and helps meet domestic and global food demand (Deschênes

and Greenstone, 2007; Paul et al., 2004). This study focuses on the Midwest because the region combines national economic importance with substantial potential for soil carbon sequestration. As Section 3 explains, I use EPIC simulations from representative Midwestern watersheds to parameterize the model, which makes this region the geographical focus of the empirical analysis.

This choice is supported by existing literature on carbon sequestration under conservation practices. Antle et al. (2001) emphasizes the economic value of soil carbon sequestration for farm income and environmental sustainability. Feng et al. (2006) compare the economic and environmental effects of land retirement and conservation practices in Iowa and underscore the region's potential. Sperow et al. (2003) quantify the economic feasibility and carbon storage potential of alternative agricultural practices, further supporting the Midwest as an appropriate setting for sequestration policy analysis.

In addition to corn and soybeans, the Midwest produces wheat, oats, barley, fruits, and vegetables, which contributes to regional economic stability and national food security. Figure 1 shows selected crops cultivated in 2022 across individual fields in the Eastern Corn Belt, a representative area with diverse soil types and climatic conditions. Given this diversity, the analysis focuses specifically on corn because of its large production area, central role in regional carbon dynamics, and sensitivity to tillage practices. Figure 2 illustrates spatial heterogeneity in soil types across the region, classified into four hydrologic groups: sandy soils (Group A), with low runoff and high infiltration; loam and silt loam soils (Group B), with moderate infiltration; clay loam soils (Group C), with lower infiltration; and clay soils (Group D), with high runoff and low infiltration. These soil characteristics directly affect SOC dynamics and yield outcomes and, in turn, shape farmers' economic incentives to adopt conservation practices.

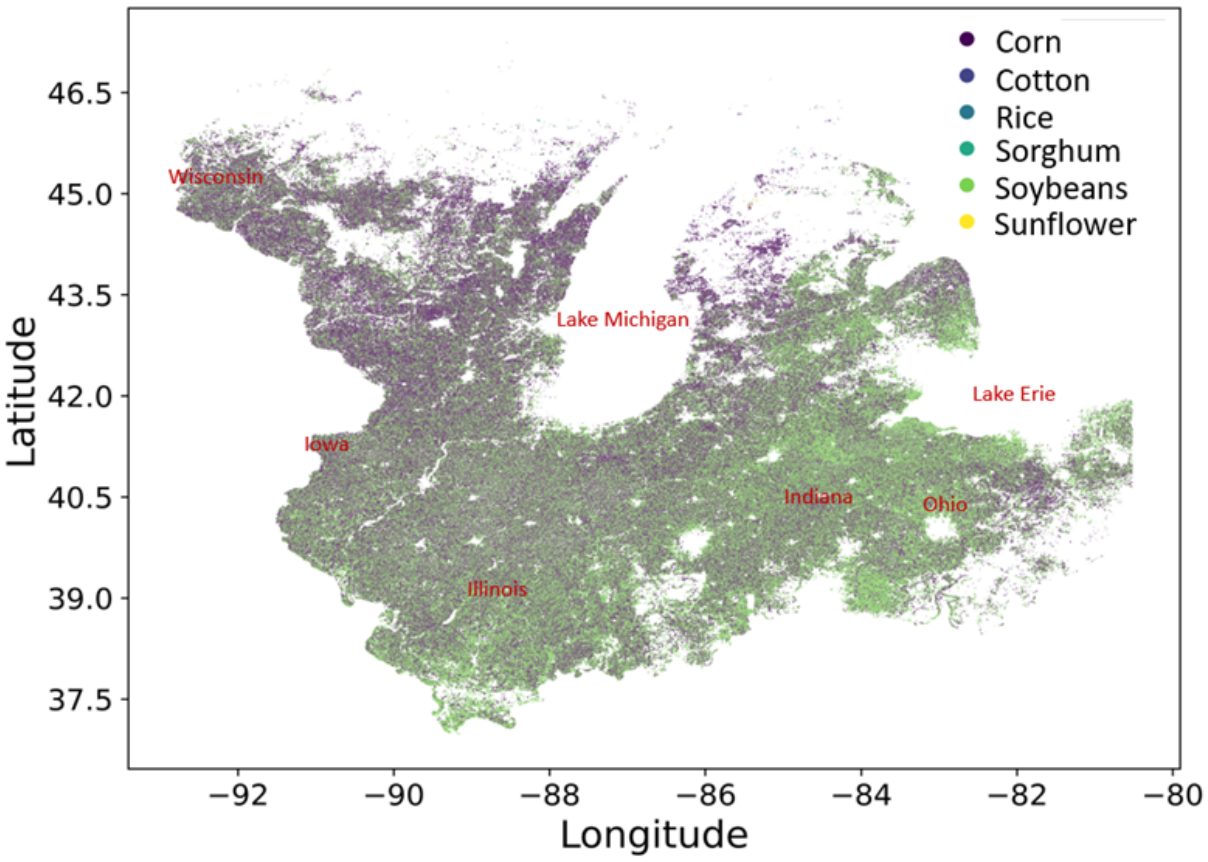


Figure 1: Major crops grown in the Eastern Corn Belt. Each point represents a field. Data are sourced from the Crop Sequence Boundaries database of the United States Department of Agriculture (USDA).

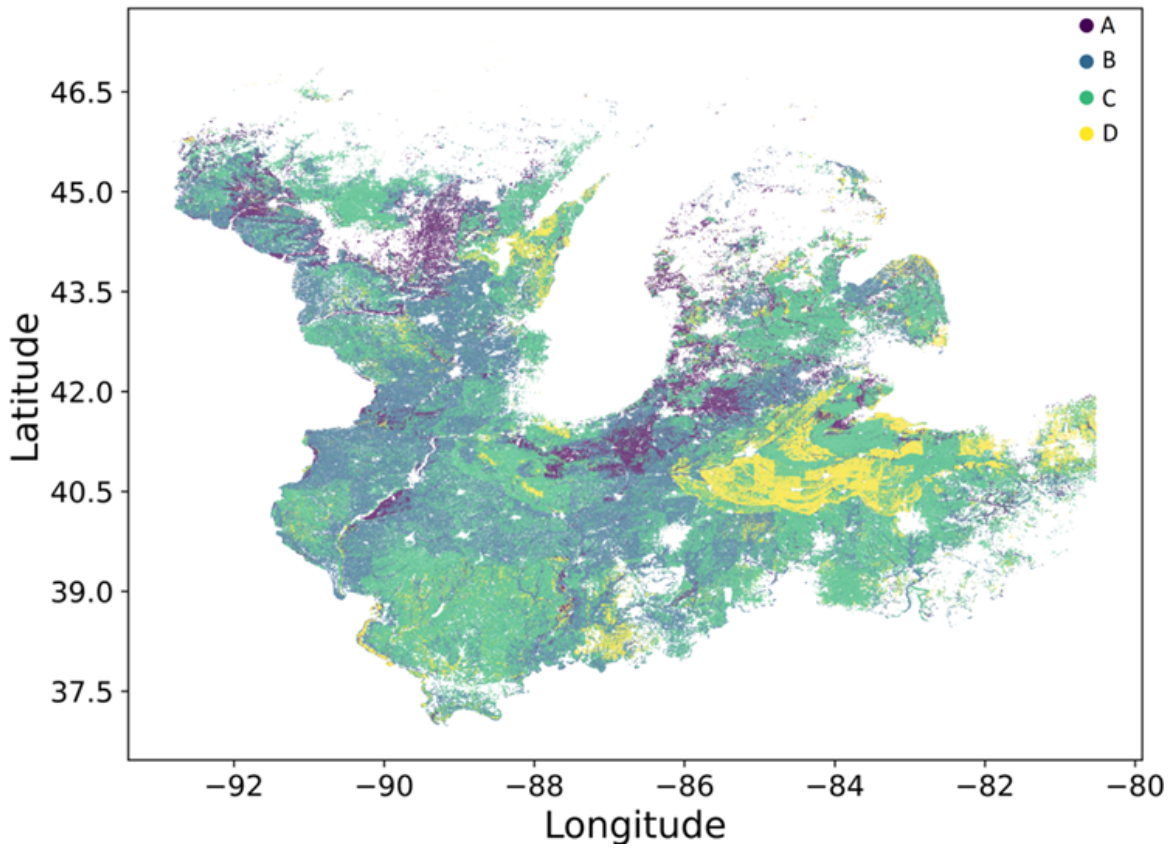


Figure 2: Soil types classified by hydrologic group in the Eastern Corn Belt region of the United States. Each point represents a field.

3 Data

I parameterize the theoretical model using simulated data from the Environmental Policy Integrated Climate (EPIC) model (Williams et al., 1989; Izaurralde et al., 2006), which integrates soil properties, climate inputs, topography, and land management decisions to simulate field-level physicochemical processes over long time horizons. Soil data are drawn from the Soil Survey Geographic Database (SSURGO), daily climate inputs from the World Climate Research Programme Coupled Model Intercomparison Project Phase 6 (CMIP6) (Eyring et al., 2016), and field boundary and land-use information from the USDA Cropland Sequence Boundaries dataset (Hunt et al., 2024). Simulation inputs comprise geospatial characteristics (latitude, longitude, slope, elevation, and aspect ratio) and daily weather variables (precipitation, minimum and maximum temperature, solar radiation, humidity, and wind speed). Soil parameters include albedo, hydrologic group, layer depth and bulk density, sand and silt fractions, pH, organic carbon content, calcium carbonate concentration, rock fragment content, and hydraulic conductivity.

Soil carbon accumulation under conservation tillage operates over horizons of 60 to 90 years, making it impractical for field experiments to observe a complete sequestration cycle within a standard research timeline. Administrative data on voluntary carbon market contracts do not yet span sufficient time to identify long-run adoption dynamics. EPIC is the standard simulation tool in the agronomic literature precisely because it has been extensively validated against observed soil carbon trajectories across diverse climatic and edaphic conditions (Izaurralde et al., 2006; Causarano et al., 2008). Importantly, the model inputs used here are drawn from real observational data. The simulation methodology is accordingly best understood as a structured integration of observational inputs through a validated biophysical process model that generates the parameter estimates needed to characterize long-run sequestration dynamics at field scale.

Management practices are standardized across simulations to isolate tillage effects. Tillage operations are scheduled in late April, corn planting in early May, and harvest in mid-

September, with residue shredded post-harvest. Annual fertilizer applications are fixed at 185 kg/ha, 150 kg/ha, and 116 kg/ha, and irrigation follows an automatic stress-triggered schedule. I evaluate three tillage systems: no-till (NT), reduced tillage (RT, tandem disk), and conventional moldboard plow tillage (CT). Fields are drawn from five representative Midwestern watersheds — Sugar, Lower Maumee, Maple, Macoupin, and Upper Fox — selected to capture soil and climate heterogeneity across the region. Within each watershed, I stratify by hydrologic soil group and sample fields proportionally, yielding 70 fields in total. Simulations are first run under CT for over 200 years until SOC reaches its long-run equilibrium value, establishing realistic baseline conditions. I then conduct 60 to 90 year simulations under NT, RT, and CT to compare SOC trajectories and crop yields. The 70-field sample is stratified by soil characteristics across five watersheds to ensure systematic coverage of the dominant soil and climate conditions in Midwestern agriculture. The market price of corn is set at \$4.04 per bushel (Macrotrends, 2024), which translates to \$160 per ton of corn (U.S. Grains Council, 2024).

Table 1 reports the key EPIC-derived parameters: C^* (ton/ha), the maximum attainable carbon stock under a given practice; C_0 (ton/ha), the baseline stock under long-run CT; s (year^{-1}), the sequestration rate; and y (ton/ha), average crop yield. NT dominates RT in both SOC sequestration and yields across all fields; the analysis accordingly focuses on the NT versus CT comparison.

4 Theoretical Framework and Results

A representative farmer chooses a tillage practice θ_t in each period to maximize expected discounted profits:

$$V = \max_{\theta_1, \theta_2, .. \theta_\infty} \sum_{t=0}^{\infty} \beta^t \mathbb{E}[\pi_t] \tag{1}$$

where $\beta \in (0, 1)$ is the discount factor. Period profits depend on the carbon payment

Table 1: Simulated mean corn yield (y, t ha^{-1}), lowest soil organic carbon (SOC) stock (C_0, t ha^{-1}), SOC threshold (C^*, t ha^{-1}), and annual carbon sequestration rate (s, yr^{-1}) under conservation tillage practices: no-till (NT), and reduced tillage (RT) for each soil hydrology group. Estimates are derived from Environmental Policy Integrated Climate (EPIC) model simulations covering 70 fields in five watersheds (Sugar Creek, Lower Maumee, Maple, Macoupin, and Upper Fox). Standard errors are in parentheses. Field-level observations appear in the Appendix.

	Yield (t ha^{-1})			Sequestration rate		Lowest SOC stock	Critical SOC threshold	
Hyd.	y_{CT}	y_{NT}	y_{RT}	s_{NT}	s_{RT}	C_0	C^*_{NT}	C^*_{RT}
A	12.04 (0.29)	11.87 (0.28)	11.79 (0.32)	0.075 (0.005)	0.078 (0.005)	32.26 (4.30)	37.51 (4.65)	36.31 (4.62)
B	11.42 (0.24)	10.49 (0.22)	10.28 (0.24)	0.058 (0.004)	0.064 (0.004)	54.31 (5.70)	65.02 (6.91)	61.85 (6.52)
C	11.15 (0.23)	10.33 (0.25)	10.14 (0.27)	0.057 (0.002)	0.067 (0.002)	53.91 (3.04)	61.91 (3.23)	59.43 (3.10)
D	11.50 (0.40)	10.79 (0.49)	10.67 (0.47)	0.060 (0.002)	0.068 (0.003)	40.46 (3.29)	46.79 (3.73)	45.25 (3.66)

Note: Standard errors in parentheses.

policy in place. I consider five alternative designs, differing in the basis of payment (carbon stock level, incremental carbon change, or conservation practice adoption) and in whether penalties apply for carbon release. The sub-sections 4.1 through 4.5 characterize each design in turn.

4.1 Policy 1: Payments proportional to the current carbon stock

Period profits are given by:

$$\pi_t = (\mathbb{E}[C_t] - C_0) \times m + \mathbb{E}[y_t] \times P - Cost(\theta_t). \tag{2}$$

Here C_t denotes the soil carbon stock at the end of period t, C_0 is the baseline carbon stock under long-run conventional tillage, m is the carbon payment rate ($ per ton of carbon), P is the crop price, y_t is crop yield, and $Cost(\theta_t)$ represents the cost associated with practice θ_t.

The farmer chooses between no-till (NT, θ_{NT}) and conventional tillage (CT, θ_{CT}), where $\theta_t \in \{\theta_{NT}, \theta_{CT}\}$. NT increases SOC over time but reduces crop yields ($y_{NT} < y_{CT}$), while CT releases carbon whenever $C_t > C_0$.

When m is sufficiently high to induce NT adoption, the value function is:

$$V_{NT} = \sum_{t=0}^{\infty} \beta^t [\mathbb{E}[y_{NT}] \times P + (\mathbb{E}[C_t] - C_o) \times m - cost(\theta_{NT})] \tag{3}$$

Following Ragot and Schubert (2008); Malik (2026), SOC sequestration dynamics under conservation practice are modeled as $\mathbb{E}[C_t] = C^* - (C^* - \tilde{C})e^{-s(t+1)}$, where s governs the sequestration rate, and depends on soil type, weather conditions, and management practices, and $\tilde{C}$ denotes the SOC at the beginning of period $t = 0$. The value function in closed-form is:

$$V_{NT} = \frac{\mathbb{E}[y_{NT}] \times P - Cost_{NT}}{1-\beta} + \frac{(C^* - C_0)m}{1-\beta} - \frac{(C^* - \tilde{C})e^{-s}m}{1-\beta e^{-s}} \tag{4}$$

When m is sufficiently low, the farmer adopts CT at all SOC levels. The initial SOC level $\tilde{C}$ decreases over time and asymptotically approaches C_o. The corresponding value function is:

$$V_{CT} = \sum_{t=0}^{\infty} \beta^t [\mathbb{E}[y_{CT}] \times P + (\mathbb{E}[C_t] - C_o) \times m - cost(\theta_{CT})] \tag{5}$$

SOC release dynamics are modeled as $\mathbb{E}[C_t] = C_0 + (\tilde{C} - C_0)e^{-s'(t+1)}$, where s' governs the release rate (Ragot and Schubert, 2008; Malik, 2026). The closed-form value function is:

$$V_{CT} = \frac{\mathbb{E}[y_{CT}] \times P - \text{Cost}_{CT}}{1-\beta} + \frac{(\tilde{C} - C_0)e^{-s'}m}{1-\beta e^{-s'}} \tag{6}$$

For the farmer to adopt NT, it must be that $V_{NT} \geq V_{CT}$, which requires:

$$m \geq \left(\frac{C^* - C_0}{1-\beta} - \frac{(C^* - \tilde{C})e^{-s}}{1-\beta e^{-s}} - \frac{(\tilde{C} - C_0)e^{-s'}}{1-\beta e^{-s'}} \right)^{-1} \left(\frac{\Delta y \times P - \Delta\text{Cost}}{1-\beta} \right) \tag{7}$$

where $\Delta y = \mathbb{E}(y_{CT} - y_{NT})$ is the expected yield loss under NT, and $\Delta Cost = cost(\theta_{CT}) - cost(\theta_{NT})$ is the difference in implementation costs. Equality in (7) defines the minimum carbon payment required to induce NT adoption.

The lifetime carbon payment per ton of sequestered carbon under NT is:

$$Payment_{NT} = \frac{m}{1-\beta} - \frac{C^* - \tilde{C}}{C^* - C_0} \frac{e^{-s} m}{1 - \beta e^{-s}} \tag{8}$$

4.2 Policy 2: Payments proportional to the carbon stock, conditional on adopting a conservation practice

In this policy, farmers receive payments proportional to their carbon stock only in periods when they adopt the conservation practice. Period profits are given by:

$$\pi_t = (\mathbb{E}[C_t] - C_0) \times m \times \mathbf{1}(\theta_t = \theta_{NT}) + \mathbb{E}[y_t] \times P - cost(\theta_t). \tag{9}$$

The key distinction from Policy 1 is that the farmer receives no carbon payment when CT is adopted, eliminating the incentive to collect payments on legacy carbon stocks without changing practices.

The value function for NT is:

$$V_{NT} = \sum_{t=0}^{\infty} \beta^t [\mathbb{E}[y_{NT}] \times P + (\mathbb{E}[C_t] - C_o) \times m - cost(\theta_{NT})] \tag{10}$$

Using the SOC dynamics for the conservation practice, the closed-form value function is:

$$V_{NT} = \frac{\mathbb{E}[y_{NT}] \times P - \text{Cost}_{NT}}{1-\beta} + \frac{(C^* - C_0)m}{1-\beta} - \frac{(C^* - \tilde{C})e^{-s} m}{1 - \beta e^{-s}} \tag{11}$$

With CT, the farmer receives no carbon payment, so the value function simplifies to:

$$V_{CT} = \sum_{t=0}^{\infty} \beta^t [\mathbb{E}[y_{CT}] \times P - cost(\theta_{CT})] = \frac{\mathbb{E}[y_{CT}] \times P - \text{Cost}_{CT}}{1-\beta} \tag{12}$$

For the farmer to adopt NT, it must be that $V_{NT} \geq V_{CT}$, which requires:

$$m \geq \left(\frac{C^* - C_o}{1-\beta} - \frac{(C^* - \tilde{C})e^{-s}}{1-\beta e^{-s}} \right)^{-1} \left(\frac{\Delta y \times P - \Delta \text{Cost}}{1-\beta} \right) \tag{13}$$

Note that m does not depend on the carbon release rate s', since the farmer receives no payment under CT regardless of the SOC trajectory. The lifetime carbon payment per ton of sequestered carbon for NT is given by equation (8).

4.3 Policy 3: Payments or penalties proportional to the incremental carbon stock

Under this policy, farmers are compensated for increases in SOC within a given period and penalized for any SOC released in periods of conventional practices. Period profits are given by:

$$\pi_t = \mathbb{E}[C_t - C_{t-1}] \times m + \mathbb{E}[y_t] \times P - cost(\theta_t) \tag{14}$$

The value function for NT is:

$$V_{NT} = \frac{(C^* - \tilde{C})(1-e^{-s})m}{1-\beta e^{-s}} + \frac{\mathbb{E}[y_{NT}] \times P - Cost_{NT}}{1-\beta} \tag{15}$$

The corresponding expression for CT is:

$$V_{CT} = \frac{(\tilde{C} - C_o)(e^{-s'} - 1)m}{1-\beta e^{-s'}} + \frac{\mathbb{E}[y_{CT}] \times P - Cost_{CT}}{1-\beta} \tag{16}$$

The condition $V_{NT} \geq V_{CT}$ requires:

$$m \geq \left(\frac{(C^* - \tilde{C})(1-e^{-s})}{1-\beta e^{-s}} + \frac{(\tilde{C} - C_0)(1-e^{-s'})}{1-\beta e^{-s'}} \right)^{-1} \frac{\Delta y \times P - \Delta Cost}{1-\beta} \tag{17}$$

The lifetime carbon payment per ton of sequestered carbon is:

$$Payment_{NT} = \frac{C^* - \tilde{C}}{C^* - C_0} \frac{(1 - e^{-s})m}{1 - \beta e^{-s}} \tag{18}$$

4.4 Policy 4: Payments proportional to the incremental carbon stock, conditional on adopting a conservation practice

This policy pays farmers proportional to the incremental increase in SOC within a given period when they adopt the conservation practice, but imposes no penalty for carbon release upon reverting to conventional tillage. Period profits are given by:

$$\pi_t = \mathbb{E}[C_t - C_{t-1}] \times m \times \mathbf{1}(\theta_t = \theta_{NT}) + \mathbb{E}[y_t] \times P - cost(\theta_t). \tag{19}$$

The value functions for NT and CT are:

$$V_{NT} = \frac{(C^* - \tilde{C})(1 - e^{-s})m}{1 - \beta e^{-s}} + \frac{\mathbb{E}[y_{NT}] \times P - Cost_{NT}}{1 - \beta} \tag{20}$$

$$V_{CT} = \frac{\mathbb{E}[y_{CT}] \times P - Cost_{CT}}{1 - \beta} \tag{21}$$

The condition $V_{NT} \geq V_{CT}$ requires:

$$m \geq \left(\frac{(C^* - \tilde{C})(1 - e^{-s})}{1 - \beta e^{-s}} \right)^{-1} \frac{\Delta y \times P - \Delta Cost}{1 - \beta} \tag{22}$$

The lifetime carbon payment per ton of sequestered carbon for NT is given by equation (18).

Result 1 (Structural cycling equilibrium under Policy 4). *For any finite payment rate m, there exists a threshold $\bar{C}(m) \in (C_0, C^*)$ beyond which NT adoption becomes unprofitable. The threshold $\bar{C}(m)$ is strictly increasing in m, but $\bar{C}(m) < C^*$ for all finite m. Consequently,*

no finite payment rate sustains permanent NT adoption, and the long-run equilibrium under Policy 4 is characterized by repeated switching between NT and CT.

Proof. For a given carbon payment rate, m, the threshold soil carbon level above which NT is no longer optimal is given by:

$$\bar{C}(m) = C^* - \frac{(\Delta y \times P - \Delta Cost)(1 - \beta e^{-s})}{m(1-\beta)(1-e^{-s})} \tag{23}$$

Differentiating (23) with respect to m yields $\partial \bar{C}(m)/\partial m > 0$, implying that the threshold increases with the payment rate. Moreover, $\bar{C}(m) < C^*$ for every finite m. As C exceeds $\bar{C}(m)$, the farmer abandons NT and switches to CT. The farmer subsequently returns to NT once soil carbon has declined sufficiently, generating repeated switching between NT and CT in the long run. Upon reaching $\bar{C}(m)$, the farmer switches to CT until the carbon level reaches C_L. Let it take t_s periods of NT to increase the carbon level back to $\bar{C}(m)$. Cycling between the carbon levels C_L and $\bar{C}(m)$ is preferred to remaining indefinitely at the threshold $\bar{C}(m)$ whenever the discounted carbon payments exceed the associated yield losses, i.e.,

$$\sum_{t=1}^{t_s} \beta^{t-1}(C^* - C_L)(e^s - 1)me^{-st} - \sum_{t=1}^{t_s} \beta^{t-1}(\Delta y \times P - \Delta Cost) \geq 0 \tag{24}$$

Also,

$$C_L = C^* - e^{st_s}(C^* - \bar{C}(m)) \tag{25}$$

Combining these equations yields the transcendental equation in t_s for which a cyclic equilibrium is profitable:

$$\frac{e^{st_s}(1 - (\beta e^{-s})^{t_s+1})}{1 - \beta^{t_s+1}} - \frac{\Delta y \times P - \Delta Cost}{(1-\beta)(C^* - \bar{C}(m))} \geq 0 \tag{26}$$

Since the second term in (26) is finite and the first term increases without bound as t_s

increases, there exists a finite t_s sufficiently large such that (26) is satisfied. Hence, repeated switching between NT and CT is profitable.

4.5 Policy 5: Payments for adopting a conservation practice

This policy pays the farmer a constant payment m in each period of conservation practice adoption, irrespective of the carbon stock level or the quantity of carbon sequestered. For the farmer to adopt NT, the payment must cover the expected yield loss and any additional adoption costs:

$$m \geq \Delta y \times P - \Delta Cost \tag{27}$$

The lifetime carbon payment per ton of sequestered carbon is:

$$payment_{NT} = \frac{m}{(C^* - C_0)(1-\beta)} \tag{28}$$

4.6 Comparative Analysis of Payment Policies

Figure 3 shows how the minimum carbon payment m varies with the initial carbon stock $\tilde{C}$ under Policies 1 through 4. Under Policies 1, 2, and 3, m is decreasing in $\tilde{C}$: farmers with higher initial carbon stocks require lower payments to adopt NT because they generate larger carbon revenues from the outset. Under Policy 4, the relationship reverses: m is strictly increasing in $\tilde{C}$, and as $\tilde{C} \to C^*$, equation (22) implies $m \to \infty$. This is the structural defection problem established in Result 1: for any fixed payment rate, farmers facing declining incremental sequestration gains rationally revert to conventional tillage to release stored carbon and restart the payment cycle. Policy 4 is therefore excluded from the welfare comparison that follows.

The welfare comparison across the remaining designs uses the discounted lifetime carbon payment as the relevant cost measure, evaluated at $\tilde{C} = C_0$, the condition that maximizes m under Policies 1, 2, and 3 and therefore provides the most conservative welfare comparison.

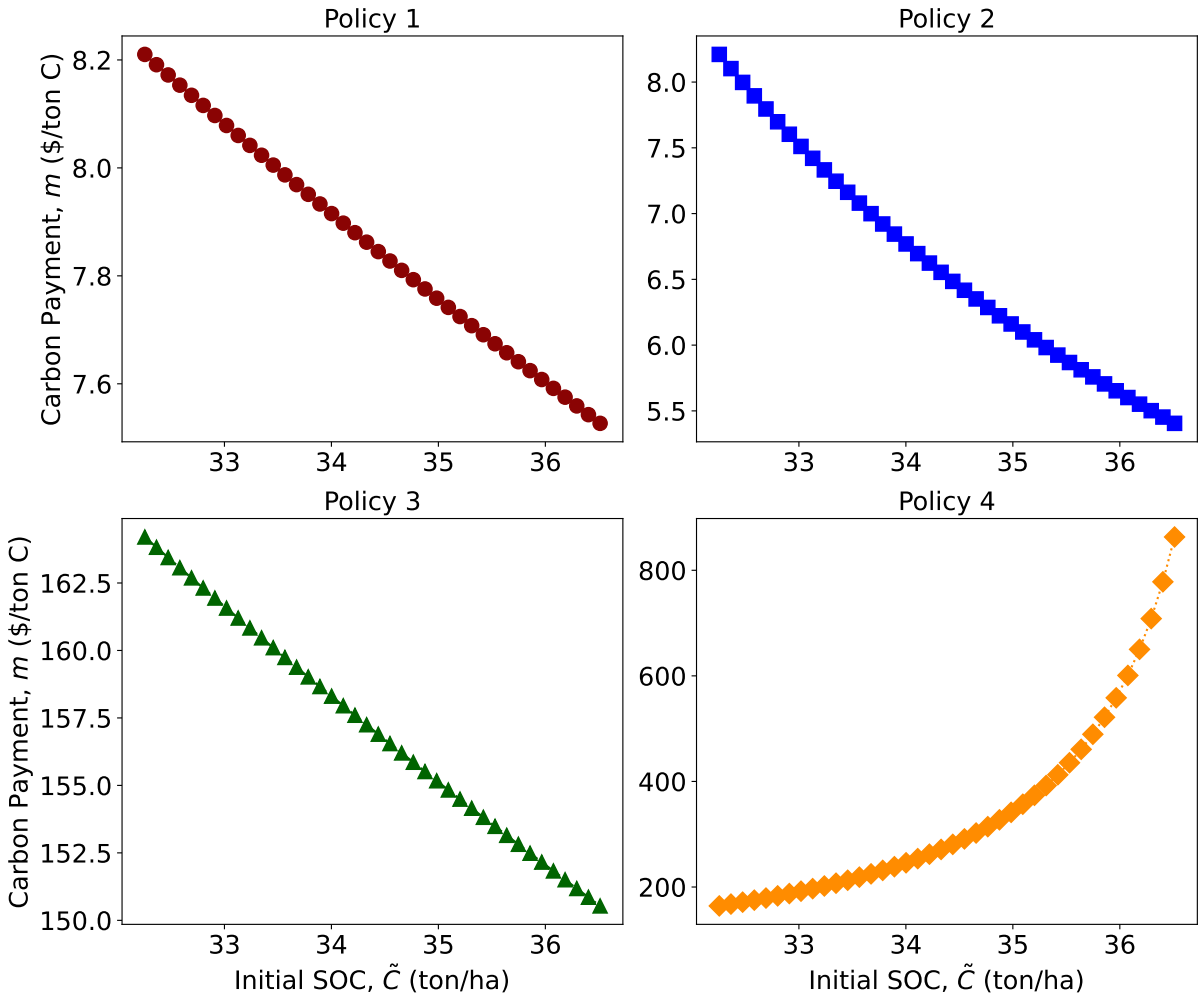


Figure 3: Minimum carbon payment m required to incentivize NT as a function of initial carbon stock $\tilde{C}$ under Policies 1 through 4, for the representative field in the best-draining soil type (hydrology group A).

Figure 4 reports these lifetime payments. Although Policy 3 requires the highest per-period m at low SOC levels, it generates the lowest lifetime payments: payments are made only on incremental SOC gains each period, and cease entirely once the carbon stock reaches its saturation level C^*. This does not, however, make Policy 3 preferable: the lock-in problem at saturation means the farmer bears continued yield costs while receiving no additional payments, making it unattractive despite low lifetime payment levels. While Policy 2 requires a lower per-period payment m than Policy 1 when $\tilde{C} > C_0$ and thus lower discounted lifetime payments, both policies generate identical discounted lifetime payments when $\tilde{C} = C_0$. The

US social cost of carbon is \$190 per ton of CO_2, equivalent to \$697 per ton of carbon (Farah and Clark, 2022). Discounted lifetime payments under Policies 1 and 2 remain below this threshold for three of the four soil types studied, confirming that these designs are welfare-improving. For the most poorly drained soil type (hydrology group D), discounted lifetime payments under Policies 1 and 2 exceed the SCC, indicating that conservation tillage on poorly drained soils may not pass a social cost-benefit test at current carbon prices.

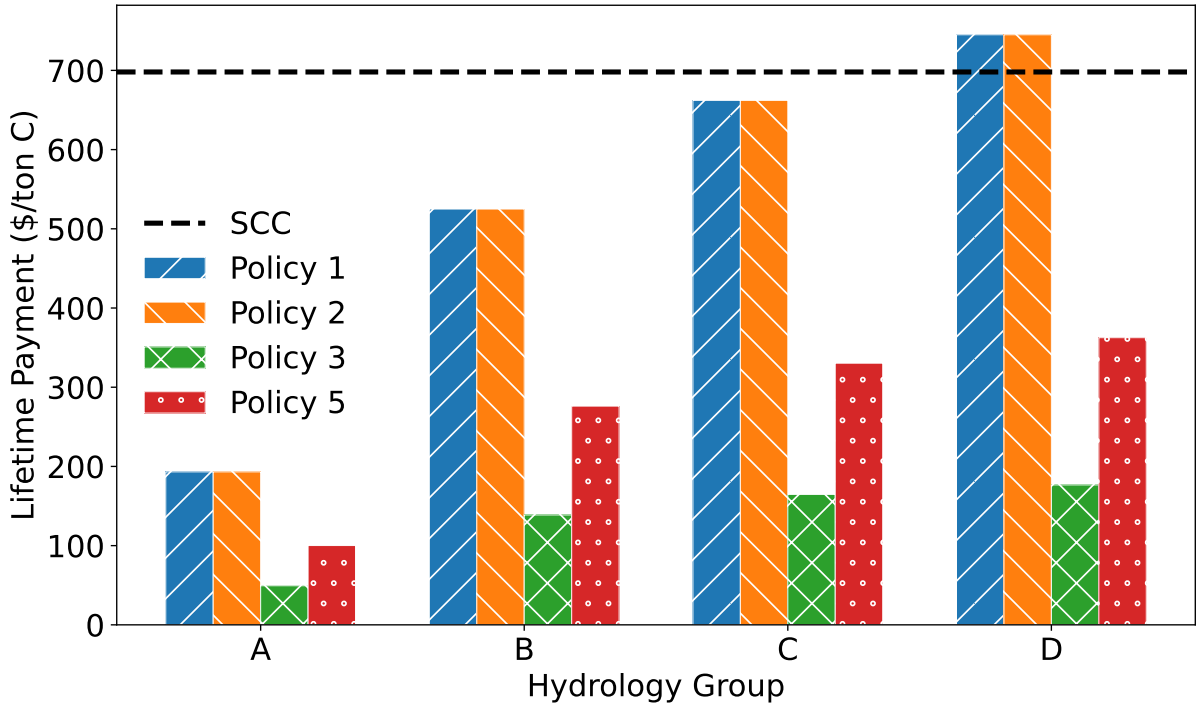


Figure 4: Discounted lifetime carbon payments for Policies 1, 2, 3, and 5 when NT is adopted and $\tilde{C} = C_0$, computed using m values obtained from the Bellman equation solution. The dashed line indicates the US social cost of carbon.

Table 2 reports m values from the analytical expressions of each policy when $\tilde{C} = C_0$. Policy 3 requires higher per-period payments m than Policies 1 and 2 because the payment is proportional to the incremental carbon gain in each period rather than the total stock. Policy 5 requires higher payments because it ignores the trajectory of carbon accumulation over time. Across all policies, m varies considerably with soil type, underscoring the importance of spatially targeted payment schemes.

Table 2: Optimal carbon payments ($/ton C) calculated using analytical expressions and from the numerical solutions of the Bellman equation for all hydrology groups.

Analytical					Bellman Equation	
Policy 1	Policy 2	Policy 3	Policy 5	Policy 1	Policy 2	Policy 3
8.21	8.21	164.20	26.31	12.00	12.00	162.00
25.38	25.38	507.61	147.78	34.00	34.00	510.00
30.59	30.59	611.84	132.19	43.00	43.00	610.00
32.84	32.84	656.73	114.74	48.00	48.00	640.00

4.7 Incorporating SOC Stochasticity Through Bellman Equation

The analytical expressions derived above abstract from stochasticity in the carbon sequestration process. I now validate these results against numerical solutions obtained by formulating the infinite-horizon optimization problem recursively through the Bellman equation. Equation (1) can be written as:

$$V(C) = \max_{\theta} \left\{ \mathbb{E}\big[\pi(C,\theta)\big] + \beta \sum_{C'} P(C' \mid C,\theta)\, V(C') \right\} \tag{29}$$

where $V(C)$ is the value function representing the maximum expected discounted profits attainable from SOC state C, θ is the management practice chosen in a given period, $\mathbb{E}[\pi(C,\theta)]$ is expected current-period profit, and $P(C' \mid C,\theta)$ is the transition probability from state C to state C' for practice θ. Transition probabilities are constructed assuming that stochastic variation in SOC is normally distributed, subject to $C \in [C_0, C^*]$. The Bellman equation is solved using value function iteration.

Assuming that the stochastic variation in the state space variable C follows normal distributions around the expected values, the value function can be expressed as:

$$V(C) = \max_{\theta} \left\{ \mathbb{E}\big[\pi(C,\theta)\big] + \beta \left[\int_{-\infty}^{\infty} \frac{e^{-(C'-\mathbb{E}(C'))^2/(2\sigma_c^2(\theta))}}{\sqrt{2\pi}\sigma_c(\theta)} V(C')dC' \right] \right\} \tag{30}$$

Since soil carbon is bounded, $C \in (C_0, C^*)$, the integral in equation (30) is adjusted as:

$$V(S) = \max_{\theta} \Bigg\{ \mathbb{E}\big[\pi(C,\theta)\big] + \beta \Bigg[\int_{-\infty}^{C_o} \phi_\theta(C')\, V(C_o)\, dC' + \int_{C_o}^{C^*} \phi_\theta(C')\, V(C')\, dC' + \int_{C^*}^{\infty} \phi_\theta(C')\, V(C')\, dC' \Bigg] \Bigg\} \tag{31}$$

where $\phi_\theta(C') = \frac{\exp\left(-\frac{(C' - \mathbb{E}(C'))^2}{2\sigma_c^2(\theta)}\right)}{\sqrt{2\pi}\,\sigma_c(\theta)}$.

The variability in soil carbon associated with practice θ is captured by $\sigma_c(\theta)$. Crop yield is also subject to stochastic variation arising from weather, soil, and field conditions. However, only its expected value enters the profit function when solving for optimal farmer decisions.

Table 2 reports optimal carbon payments from both the analytical expressions and the Bellman equation solutions. For Policies 1 and 2, Bellman-derived m values are slightly higher than their analytical counterparts, reflecting the additional compensation required to offset uncertainty in carbon sequestration outcomes. For Policy 3, the numerical and analytical solutions converge closely. Across all policies, m varies substantially with soil type, confirming that cost-effective program design calls for spatially targeted payments calibrated to biophysical characteristics.

Figure 5 illustrates optimal farmer decisions as a function of SOC for the representative field in the best draining soil type (hydrology group A). With Policy 2, farmers adopt CT at all SOC levels when $m \leq \$5/ton\ C$. For payment rates between \$6 and \$11 per ton C, farmers adopt CT for small $\tilde{C}$ and switch to NT for higher $\tilde{C}$. For $m \geq \$12/ton\ C$, NT is optimal at all SOC levels. Farmer behavior with Policy 1 is qualitatively similar.

In Policy 3, farmer behavior exhibits a richer pattern consistent with the lock-in problem identified in Section 4.3. For $m < \$162/ton\ C$, farmers adopt NT for small $\tilde{C}$ where sequestration rates are high and incremental payments are large. At intermediate $\tilde{C}$, as the

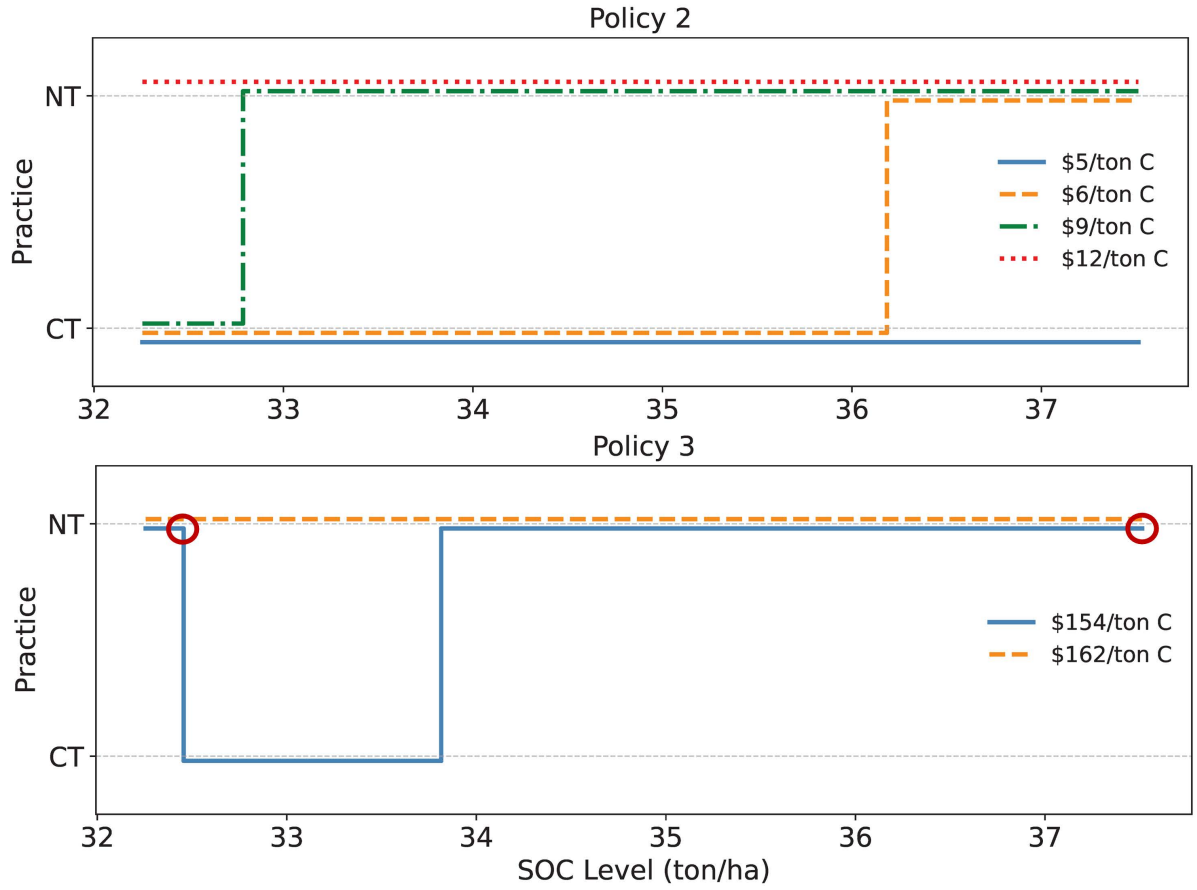


Figure 5: Optimal farmer decisions for the representative field in the best draining soil type (hydrology group A) under Policies 2 and 3 for different values of m. Red circles indicate the two equilibrium points under Policy 3.

sequestration rate slows, farmers revert to CT. At high $\tilde{C}$, the penalty for carbon release is sufficiently large to make NT optimal again. This generates two equilibrium points, indicated by the red circles in Figure 5: a lower equilibrium at $\tilde{C}_1 = 32.44$ tons C, where the farmer switches from NT-to-CT, and an upper equilibrium at $\tilde{C}_2 = C^*$. The reverse switch from CT-to-NT occurs at $\tilde{C} = 33.81$ tons C. Farmers with $\tilde{C} < 33.81$ tons C sequester carbon up to $\tilde{C}_1$; those with higher initial stocks sequester to saturation at $\tilde{C}_2$.

4.8 Policy Ranking and Additionality

The analysis yields a clear policy ranking. Policy 4 is eliminated by Result 1: the cycling equilibrium ensures that participating farmers rationally defect to conventional tillage as their carbon stock rises, producing zero net permanent sequestration for any finite payment rate. Policy 3, despite generating the lowest discounted lifetime payments, is unlikely to achieve sustained adoption in practice. The penalty for carbon release is politically and administratively costly to implement, and once soils reach their saturation level C^*, payments cease while farmers continue to bear yield losses from conservation practices and face prohibitive penalties for reverting to conventional tillage. The lock-in problem makes Policy 3 unattractive to farmers regardless of payment levels. Policy 5 is sub-optimal from a social planner's perspective: because payments are tied to practice adoption rather than carbon outcomes, there is no accountability for actual sequestration, and farmers may engage in operations that release stored carbon while nominally maintaining conservation practices.

Policy 2 dominates Policy 1 on additionality grounds. In Policy 1, a farmer with a high legacy carbon stock who adopts conventional tillage continues to collect carbon payments proportional to that stock, generating inframarginal transfers with no associated sequestration. With Policy 2, payments are conditional on conservation practice adoption, which eliminates this incentive entirely. Policy 2 is therefore the optimal design: it minimizes required payment levels, maintains consistent adoption incentives throughout the sequestration horizon, and substantially limits the additionality problem.

A farmer is inframarginal, that is, adopts NT in the absence of any carbon payment, if and only if $\Delta y \leq \Delta Cost$. With the maintained assumption that implementation cost differences are negligible, this condition reduces to $\Delta y \leq 0$: the farmer's yield does not decline under NT relative to CT. Of the 70 fields in the EPIC sample, two satisfy $\Delta y \leq 0$, indicating that non-additional participation is limited in the present sample but non-negligible in practice. Field-level results are reported in the Appendix. Under Policy 2, such farmers receive payments only when they adopt NT, which limits but does not eliminate the welfare

cost of non-additional transfers relative to the social optimum. In Policy 1, inframarginal farmers collect payments regardless of practice, making the additionality problem strictly worse.

4.9 Welfare Gains from Spatially Targeted Carbon Payments

The variation in required payment rates across soil types documented above implies that a uniform national carbon price is welfare-inferior to a spatially targeted scheme calibrated to soil characteristics. I quantify this welfare gap using the cost structure of Policy 2, the optimal design identified in Section 4.8, evaluated across the agricultural land of the five watersheds studied. Table 3 reports the total agricultural area, lifetime payment per ton of carbon, SOC gain per hectare, total SOC gain, and total program cost for each hydrology group. Spatially targeted payments calibrated to each soil type imply a cumulative lifetime program cost of $5.19 billion for a total carbon sequestration of 9.008 million tons, or $576.4 per ton C. This is substantially below the US social cost of carbon of $697 per ton C (Farah and Clark, 2022), confirming that the targeted policy is welfare-improving. A uniform payment scheme set at $48 per ton C, the rate required to induce adoption on the most costly soil type, implies a sequestration cost of $745 per ton of carbon, slightly exceeding the SCC. Spatially targeted payments therefore reduce total program costs by approximately 22% relative to the uniform scheme while achieving the same sequestration outcome.

Table 3: Cost analysis of spatially targeted carbon payments for Policy 2 across the agricultural land of the five watersheds. Lifetime payments are calibrated to each soil type's biophysical characteristics.

Hydrology	Area (ha)	Lifetime payment ($/ton C)	ΔSOC/Area (ton ha^{-1})	ΔSOC (million tons)	Cost (million $)
A	96,609	193.13	5.26	0.508	98.11
B	382,155	524.97	10.70	4.089	2146.62
C	510,008	662.14	8.00	4.080	2701.54
D	52,307	744.99	6.33	0.331	246.59
Total	1,041,079			9.008	5192.86

5 Breakeven Point and Front Loaded Payment Schemes

This section focuses exclusively on Policy 2, which the preceding analysis identifies as the optimal design. For any payment level m, there exists a breakeven time T of net profits determined by:

$$\sum_{t=0}^{T} \beta^t \left[(\Delta y \times P - (C^* - C_0)(1 - e^{-s(t+1)})m - \Delta Cost \right] = 0 \tag{32}$$

The closed-form expression is:

$$\frac{(\Delta y \times P - \Delta \text{Cost})(1 - \beta^{T+1})}{1 - \beta} - \left[\frac{1 - \beta^{T+1}}{1 - \beta} - \frac{\left[1 - (\beta e^{-s})^{T+1}\right] e^{-s}}{1 - \beta e^{-s}} \right] (C^* - C_o)m = 0 \tag{33}$$

At the minimum payment level derived in (13), the breakeven time is infinite. Figure 6 illustrates this relationship for a representative field in the best-draining soil type (hydrology group A). A marginal increase above the minimum m yields 35 years to breakeven, and reducing this horizon to fewer than 5 years requires approximately four times larger payments than the minimum value.

The above analysis with a constant carbon payment rate leads to long payback periods, reducing the attractiveness of adoption of conservation practices. A natural alternative is a time-varying payment scheme that front-loads payments. Let $m(t)$ denote the payment at time t, with $\lim_{t\to\infty} m(t) = m_\infty$. For adoption to remain optimal at the saturation SOC level C^*, m_∞ must satisfy:

$$m_\infty \geq \frac{\Delta y \times P - \Delta \text{Cost}}{C^* - C_0} \tag{34}$$

Table 4 reports m_∞ for the representative fields of different hydrology groups. The minimum payment schedule balances the lifetime profits from NT adoption with those from

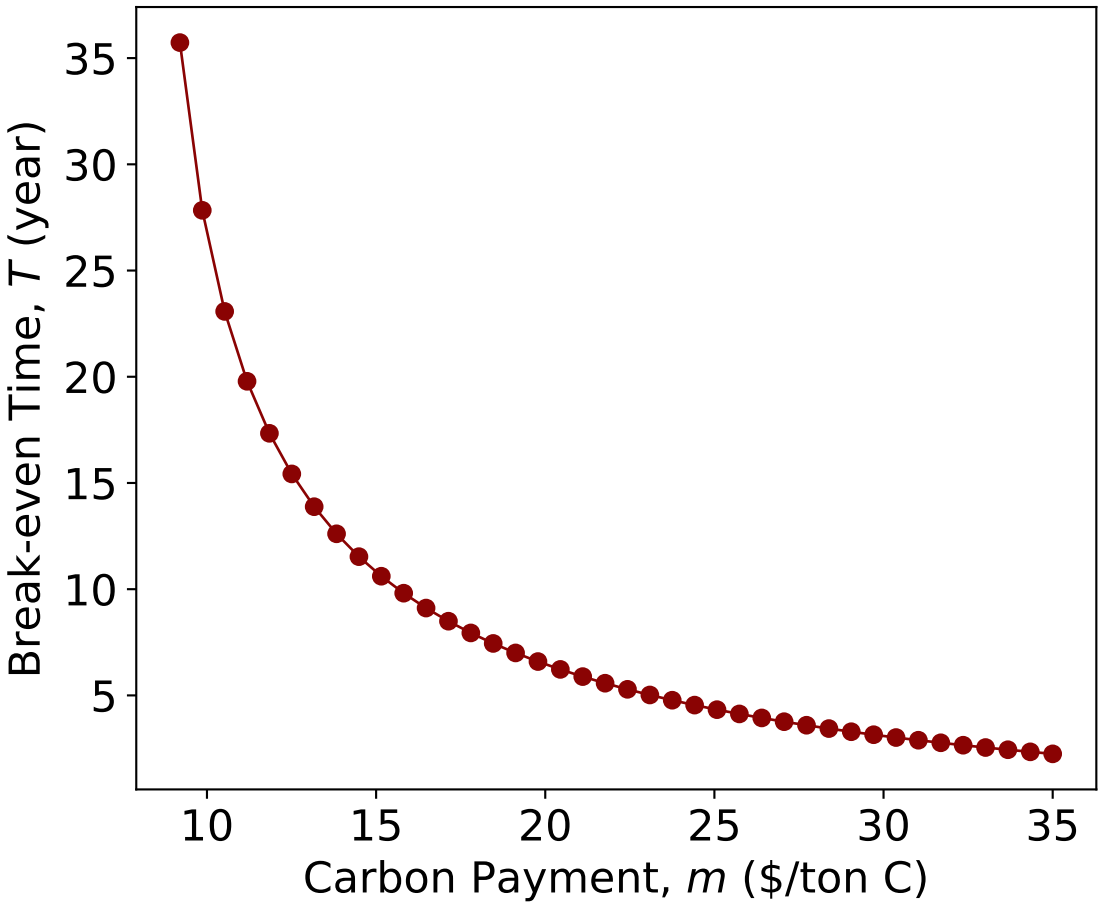


Figure 6: Breakeven time T as a function of the carbon payment m for a representative field in best-draining soil type (hydrology group A).

CT, and thus satisfies:

$$\sum_{t=0}^{\infty} \beta^t \left[\mathbb{E}(y_{NT}) \times P + (C^* - C_0)(1 - e^{-s(t+1)}) m(t) - \text{Cost}_{NT} \right] = \sum_{t=0}^{\infty} \beta^t \left[\mathbb{E}(y_{CT}) \times P - \text{Cost}_{CT} \right] \tag{35}$$

Table 4: Minimum carbon payment m and limiting payments m_∞ by hydrology group. All values are in units of \$/ton C.

Hydrology	m	m_∞
A	8.21	5.01
B	25.38	13.81
C	30.59	16.52
D	32.84	18.13

Equation (35) reveals that all optimal payment schedules $m(t)$ yield identical lifetime discounted payments, given by the expression $\sum_{t=0}^{\infty} \beta^t (C^* - C_0)(1 - e^{-s(t+1)}) m(t)$. As an example of a front-loaded carbon payment scheme, one can consider the functional form $m(t) = ae^{-bt} + m_\infty$. In this scheme, $m(0) = a + m_{infty}$ and the payment decreases and asymptotically approaches m_∞ with time. Parameter b decides the rate of decline of the payment. Substituting into (35) yields:

$$\frac{a}{1 - \beta e^{-b}} - \frac{a e^{-s}}{1 - \beta e^{-(s+b)}} = \frac{\Delta y \times P - \Delta \text{Cost}}{(1 - \beta)(C^* - C_0)} - \frac{m_\infty}{1 - \beta} + \frac{m_\infty e^{-s}}{1 - \beta e^{-s}} \tag{36}$$

Using the m_∞ relation given in equation (34), one gets:

$$a = \left[\frac{1}{1 - \beta e^{-b}} - \frac{e^{-s}}{1 - \beta e^{-(s+b)}} \right]^{-1} \times \frac{m_\infty e^{-s}}{1 - \beta e^{-s}} \tag{37}$$

The breakeven time T under this time-varying payment scheme is given by substituting *m(t)* in equation 32:

$$\sum_{t=0}^{T} \beta^t \left[(\Delta y \times P - (C^* - C_0)(1 - e^{-s(t+1)})(ae^{-bt} + m_\infty) - \Delta Cost \right] = 0 \tag{38}$$

The corresponding closed-form expression becomes:

$$a\frac{1-(\beta e^{-b})^{T+1}}{1-\beta e^{-b}} - ae^{-s}\frac{1-(\beta e^{-(s+b)})^{T+1}}{1-\beta e^{-(s+b)}} - m_\infty e^{-s}\frac{1-(\beta e^{-s})^{T+1}}{1-\beta e^{-s}} = 0 \tag{39}$$

Front-loaded payments, however, introduce a defection incentive: farmers may revert to conventional tillage once payments decline over time. To prevent this, payments must remain above the level that makes deviation in any period unprofitable. For a time-period t, this threshold payment level, $m_s(t)$ is given by:

$$m_s(t) = \frac{\Delta y \times P - \Delta Cost}{(C^* - C_o)(1 - e^{-s(t+1)})} \tag{40}$$

Proposition 1. *The threshold payment level, $m_s(t)$ is an optimal payment scheme.*

Proof: $m_s(t)$ satisfies equation (35) and is therefore an optimal payment scheme.

Since $m_s(t)$ is an optimal payment scheme, any schedule that never intersects it constitutes either an over- or an underpayment, implying that an optimal payment scheme must intersect $m_s(t)$ at least once. A payment schedule is incentive-compatible if this crossing occurs exactly once, and $m(t=0) \leq m_s(t=0)$, ensuring that beyond the intersection point the farmer has no incentive to revert to conventional tillage. Proposition 2 establishes that this condition holds when the rate of decay of front-loaded payments b does not exceed the carbon sequestration rate s.

Proposition 2. *A payment schedule $m(t) = ae^{-bt} + m_\infty$ is incentive-compatible if $a(e^s - 1) < m_\infty$ and $b \leq s$.*

Proof: The first condition, $a(e^s - 1) < m_\infty$ is directly derived from the requirement that $m(0) \leq m_s(0)$.

Let t^* denote the time for which $m(t^*) = m_s(t^*)$. The desired behavior is that $m(t) < m_s(t)$ for $t < t^*$ and $m(t) > m_s(t)$ for $t > t^*$. Consider the function $g(t) = m(t) - m_s(t)$.

Now,

$$g(t) = ae^{-bt} + m_\infty - \frac{m_\infty}{1 - e^{-s(t+1)}}$$
$$\implies g(t) = \frac{ae^{-bt}(e^{s(t+1)} - 1) - m_\infty}{e^{s(t+1)} - 1}$$

Since the denominator of $g(t)$ is always positive, consider the numerator:

$$F(t) = ae^s e^{(s-b)t} - ae^{-bt} - m_\infty$$
$$\implies F'(t) = a[e^s(s-b)e^{(s-b)t} + be^{-bt}]$$

Thus, *F(t)* is a monotonically increasing function when $b \leq s$. Hence, there is only one critical point. This proves the proposition.

The critical point, t^* obtained by $F'(t) = 0$ is given by:

$$t^* = \frac{1}{s} ln \left(\frac{b}{b-s} \right) - 1$$

The condition $b > s$ implies that $t^* \in \mathbb{R}$.

To illustrate how the front-loaded payments reduce breakeven times, consider the payment schemes in which the optimal values of a, obtained from equation (37) for different values of b, are increased by \$2 to obtain a finite breakeven time. Figure 7 shows these payment paths along with $m_s(t)$ and the flat payment scheme ($b = 0$). The associated breakeven times are marked as red diamonds. The breakeven times decline from 25 years for $b = 0$ to 16 years for $b = s$, which is a significant reduction. The breakeven times can be further reduced by choosing a larger value of a. Figure 7 also shows that after the initial time periods, the payment schemes remain larger than $m_s(t)$ and thus are incentive-compatible.

Lastly, Proposition 3 demonstrates that the parameter a of the optimal front-loaded payment scheme, which dictates the front-loaded payment levels, is bounded over the domain $b \in [0, \infty)$.

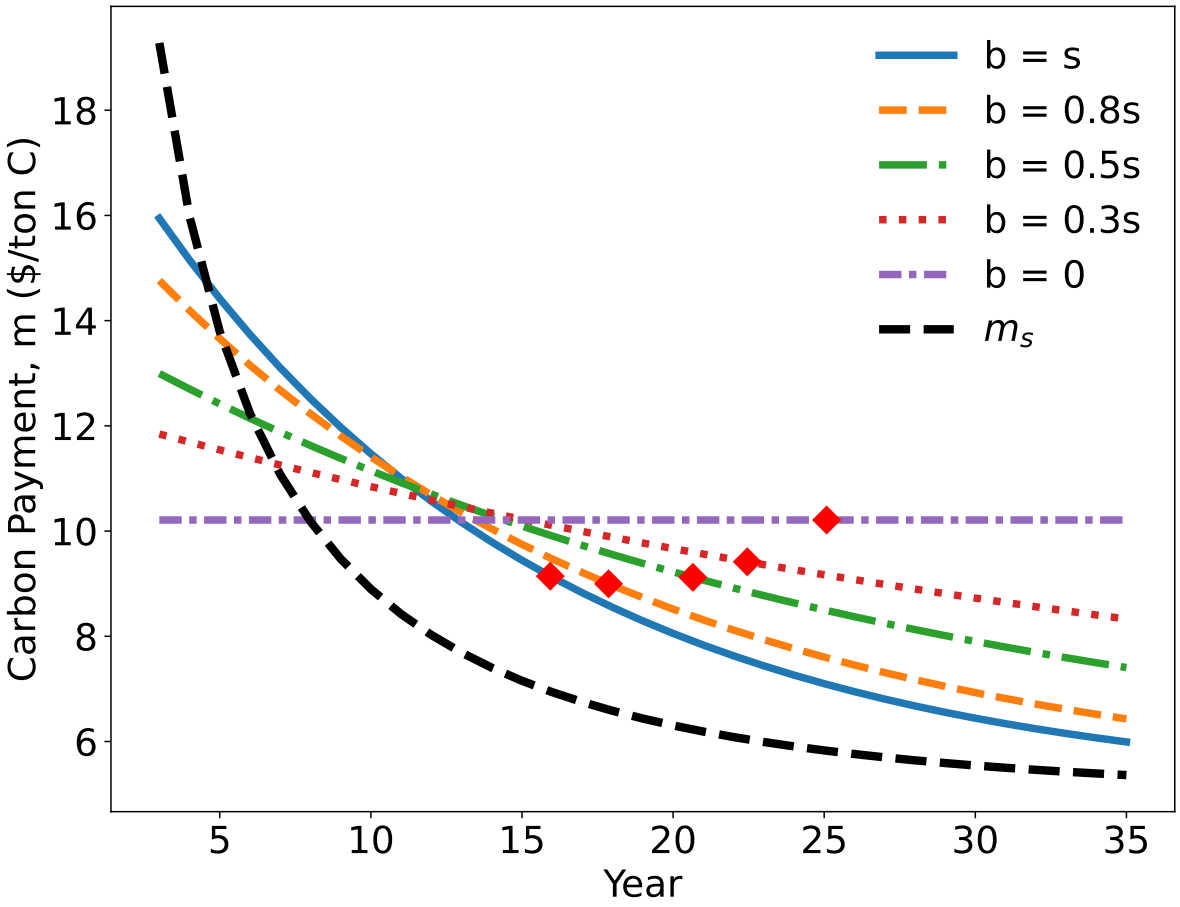


Figure 7: Front-loaded carbon payment paths of the form $m(t) = ae^{-bt} + m_\infty$ for different values of b for a representative field in the best-draining soil type (hydrology group A). a is chosen in each case as the optimal value obtained through the equation (37) plus \$2 to ensure that breakeven times are finite. Red diamond markers indicate the corresponding breakeven time for each $m(t)$.

Proposition 3. *In the optimal payment scheme,* $m(t) = ae^{-bt} + m_\infty$*, the parameter* a *satisfies:*

$$a \in \left[\frac{m_\infty e^{-s}(1-\beta)}{1-e^{-s}}, \frac{m_\infty e^{-s}}{(1-\beta e^{-s})(1-e^{-s})} \right)$$

Proof: From (37), it is deduced that a is a monotonically increasing function of b. Hence, the lower bound is attained at $b = 0$ and the upper bound is approached as $b \to \infty$.

Proposition 3 shows that the bounds of a are decreasing with s, which implies that technologies or processes that accelerate the rate of sequestration also reduce the "degree of front-loadedness" of the optimal payment scheme. Intuitively, when sequestration is rapid, the benefits of participation accrue earlier in the project life-cycle, reducing the need to compensate farmers through large up-front payments. Slower sequestration, by contrast, requires more aggressive front-loading to offset the delayed accrual of benefits.

6 Conclusion

This paper develops an analytically tractable framework to evaluate five carbon payment designs for incentivizing soil organic carbon sequestration through conservation tillage, deriving closed-form minimum payment conditions under each design and parameterizing the model using EPIC simulations across 70 Midwestern fields. The findings establish a clear ranking across payment designs. Flat adoption payments (Policy 5) are sub-optimal because they provide no accountability for actual sequestration outcomes and generate substantial inframarginal transfers. Incremental payment designs fail more fundamentally. Without penalties for carbon release (Policy 4), the minimum payment required to sustain no-till adoption is strictly increasing in the current SOC stock, generating a structural cycling equilibrium in which farmers rationally alternate between no-till and conventional tillage, with net permanent sequestration equal to zero for any finite payment rate. With penalties (Policy 3), the cycling incentive is suppressed but replaced by a lock-in problem at saturation where farmers bear continued yield costs while receiving no additional payments.

Stock-based payments conditional on conservation practice adoption (Policy 2) emerge as the uniquely robust design: required payment levels are lowest across all soil types, the additionality problem is structurally resolved by conditioning on practice adoption, and consistent sequestration incentives are maintained throughout the carbon accumulation horizon. Lifetime discounted payments under Policy 2 remain below the US social cost of carbon for three of the four soil types studied, confirming that the policy is welfare-improving. The required payment rate varies substantially with biophysical conditions. Spatially targeted payments calibrated to soil hydrology group characteristics reduce total program costs by approximately 22% relative to a uniform national carbon price while achieving equivalent sequestration, with welfare gains concentrated on well-drained soils where required payments are low. Lastly, front-loaded payment schemes can significantly shorten breakeven periods relative to flat payments, facilitating adoption. This work uncovers the conditions under which front-loaded schemes remain incentive-compatible as the payment stream diminishes, preventing farmer defection to conventional practices.

Although the model is calibrated to Midwestern field conditions, the analytical results are not specific to that context. The structural cycling equilibrium under Policy 4, the additionality problem under Policy 1, and the dominance of Policy 2 follow from the mathematics of carbon stock dynamics under forward-looking farmer optimization. These properties hold for any setting in which sequestration is reversible, soils have finite storage capacity, and conservation practices impose short-run yield costs. Voluntary carbon markets are expanding rapidly across Sub-Saharan Africa and South Asia, where additionality concerns, monitoring constraints, and farmer distrust of payment institutions pose greater implementation challenges than in the United States. In these contexts, the policy hierarchy identified here carries direct practical relevance, and the closed-form minimum payment conditions derived under Policy 2 provide a tractable basis for calibrating carbon payment programs to local biophysical and economic conditions in data-scarce environments. These findings carry direct implications for the design of conservation incentive programs and voluntary carbon

markets where payment structures remain actively debated.

7 Declaration of competing interest

The author declares no potential conflict of interest

References

Antle, J., S. Capalbo, S. Mooney, E. Elliott, and K. Paustian (2003). Spatial heterogeneity, contract design, and the efficiency of carbon sequestration policies for agriculture. *Journal of environmental economics and management 46*(2), 231–250.

Antle, J. M., S. M. Capalbo, S. Mooney, E. T. Elliott, and K. H. Paustian (2001). Economic analysis of agricultural soil carbon sequestration: an integrated assessment approach. *Journal of agricultural and resource economics*, 344–367.

Aspelund, K. M. and A. Russo (2026, February). Additionality and asymmetric information in environmental markets: Evidence from conservation auctions. Working Paper. Available at https://annarusso.github.io/papers/aspelund_russo_crp.pdf.

Berazneva, J., J. M. Conrad, D. T. Güereña, J. Lehmann, and D. Woolf (2019). Agricultural productivity and soil carbon dynamics: A bioeconomic model. *American Journal of Agricultural Economics 101*(4), 1021–1046.

Blevins, R., G. Thomas, and P. Cornelius (1977). Influence of no-tillage and nitrogen fertilization on certain soil properties after 5 years of continuous corn 1. *Agronomy journal 69*(3), 383–386.

Burt, O. R. (1981). Farm level economics of soil conservation in the palouse area of the northwest. *American journal of agricultural economics 63*(1), 83–92.

Causarano, H. J., P. C. Doraiswamy, G. W. McCarty, J. L. Hatfield, S. Milak, and A. J. Stern (2008). Epic modeling of soil organic carbon sequestration in croplands of iowa. *Journal of environmental quality 37*(4), 1345–1353.

Chen, S., D. Arrouays, D. A. Angers, M. P. Martin, and C. Walter (2019). Soil carbon stocks under different land uses and the applicability of the soil carbon saturation concept. *Soil and Tillage Research 188*, 53–58.

Deschênes, O. and M. Greenstone (2007). The economic impacts of climate change: evidence from agricultural output and random fluctuations in weather. *American economic review 97*(1), 354–385.

Eyring, V., S. Bony, G. A. Meehl, C. A. Senior, B. Stevens, R. J. Stouffer, and K. E. Taylor (2016). Overview of the coupled model intercomparison project phase 6 (cmip6) experimental design and organization. *Geoscientific Model Development 9*(5), 1937–1958.

Farah, N. H. and L. Clark (2022). Epa floats sharply increased social cost of carbon. Accessed: 2026-03-25.

Feng, H., L. A. Kurkalova, C. L. Kling, and P. W. Gassman (2006). Environmental conservation in agriculture: land retirement vs. changing practices on working land. *Journal of Environmental Economics and Management 52*(2), 600–614.

Feng, H., J. Zhao, and C. L. Kling (2002). The time path and implementation of carbon sequestration. *American Journal of Agricultural Economics 84*(1), 134–149.

Griscom, B. W., J. Adams, P. W. Ellis, R. A. Houghton, G. Lomax, D. A. Miteva, W. H. Schlesinger, D. Shoch, J. V. Siikamäki, P. Smith, et al. (2017). Natural climate solutions. *Proceedings of the National Academy of Sciences 114*(44), 11645–11650.

Gulati, S. and J. Vercammen (2005). The optimal length of an agricultural carbon contract.

Canadian Journal of Agricultural Economics/Revue canadienne d'agroeconomie 53(4), 359–373.

Gulati, S. and J. Vercammen (2006). Time inconsistent resource conservation contracts. *Journal of Environmental Economics and Management 52*(1), 454–468.

Horowitz, J., R. Ebel, and K. Ueda (2010, November). "No-Till" farming is a growing practice. Economic Information Bulletin EIB-70, U.S. Department of Agriculture, Economic Research Service. Accessed: July 1, 2026.

Hunt, K. A., J. Abernethy, P. C. Beeson, M. Bowman, S. Wallander, and R. Williams (2024). Crop sequence boundaries using usda national agricultural statistics service historic cropland data layers. *Statistical Journal of the IAOS 40*(2), 237–246.

Ismail, I., R. Blevins, and W. Frye (1994). Long-term no-tillage effects on soil properties and continuous corn yields. *Soil Science Society of America Journal 58*(1), 193–198.

Izaurralde, R., J. R. Williams, W. B. McGill, N. J. Rosenberg, and M. Q. Jakas (2006). Simulating soil c dynamics with epic: Model description and testing against long-term data. *Ecological Modelling 192*(3-4), 362–384.

Jack, B. K., S. Jayachandran, N. Kala, and R. Pande (2025). Money (not) to burn: payments for ecosystem services to reduce crop residue burning. *American Economic Review: Insights 7*(1), 39–55.

Jayachandran, S., J. De Laat, E. F. Lambin, C. Y. Stanton, R. Audy, and N. E. Thomas (2017). Cash for carbon: A randomized trial of payments for ecosystem services to reduce deforestation. *Science 357*(6348), 267–273.

Kim, M.-K., B. A. McCarl, and B. C. Murray (2008). Permanence discounting for land-based carbon sequestration. *Ecological Economics 64*(4), 763–769.

Lichtenberg, E. (2024). Thinking about soil health: A conceptual framework. *Soil Security 14*, 100130.

Macrotrends (2024). Corn prices – 59 year historical chart. Last modified: July 2024. Accessed: July 1, 2024.

Malik, K. (2026). Farmer adoption and payment design under risk: Variability in soil carbon sequestration across conservation practices. Technical report, National Bureau of Economic Research.

McConnell, K. E. (1983). An economic model of soil conservation. *American journal of agricultural economics 65*(1), 83–89.

Murray, B. C., B. Sohngen, and M. T. Ross (2007). Economic consequences of consideration of permanence, leakage and additionality for soil carbon sequestration projects. *Climatic change 80*(1), 127–143.

Paul, C., R. Nehring, D. Banker, and A. Somwaru (2004). Scale economies and efficiency in us agriculture: are traditional farms history? *Journal of Productivity Analysis 22*(3), 185–205.

Paustian, K., J. Lehmann, S. Ogle, D. Reay, G. P. Robertson, and P. Smith (2016). Climate-smart soils. *Nature 532*(7597), 49–57.

Ragot, L. and K. Schubert (2008). The optimal carbon sequestration in agricultural soils: do the dynamics of the physical process matter? *Journal of Economic Dynamics and Control 32*(12), 3847–3865.

Raina, N., M. Zavalloni, and D. Viaggi (2024). Incentive mechanisms of carbon farming contracts: A systematic mapping study. *Journal of Environmental Management 352*, 120126.

Raj Kunwar, S., R. G. Chambers, L. F. Gentry, and T. Serra (2025). What are the carbon services from cover-crop adoption worth from farmers' perspective? *American Journal of Agricultural Economics*.

Roe, S., C. Streck, R. Beach, J. Busch, M. Chapman, V. Daioglou, A. Deppermann, J. Doelman, J. Emmet-Booth, J. Engelmann, et al. (2021). Land-based measures to mitigate climate change: Potential and feasibility by country. *Global Change Biology 27*(23), 6025–6058.

Ruseva, T., J. Hedrick, G. Marland, H. Tovar, C. Sabou, and E. Besombes (2020). Rethinking standards of permanence for terrestrial and coastal carbon: implications for governance and sustainability. *Current Opinion in Environmental Sustainability 45*, 69–77.

Sadatshojaei, E., D. A. Wood, and M. R. Rahimpour (2021). Potential and challenges of carbon sequestration in soils. *Applied soil chemistry*, 1–21.

Sawadgo, W. and A. Plastina (2022). The invisible elephant. *Choices 37*(1), 1–13.

Sperow, M., M. Eve, and K. Paustian (2003). Potential soil c sequestration on us agricultural soils. *Climatic Change 57*, 319–339.

Stewart, C. E., K. Paustian, R. T. Conant, A. F. Plante, and J. Six (2007). Soil carbon saturation: concept, evidence and evaluation. *Biogeochemistry 86*, 19–31.

U.S. Grains Council (2024). Converting grain units. Last Modified: 2024. Accessed: September 12, 2024.

West, T. O. and J. Six (2007). Considering the influence of sequestration duration and carbon saturation on estimates of soil carbon capacity. *Climatic change 80*(1), 25–41.

Westcott, P. (2010). *USDA agricultural projections to 2019*. DIANE Publishing.

Williams, J., C. Jones, J. Kiniry, and D. A. Spanel (1989). The epic crop growth model. *Transactions of the ASAE 32*(2), 497–0511.

A Appendix

A.1 Derivation of carbon sequestration and release dynamics

A.1.1 Carbon sequestration

Carbon sequestration dynamics should satisfy the following boundary conditions:

$$\lim_{t\to\infty} C(t) = C^* \tag{A1}$$

$$\lim_{t\to 0} C(t) = \tilde{C} \tag{A2}$$

Carbon content asymptotically approaches the saturation value as $t \to \infty$. Hence,

$$\lim_{t\to\infty} \frac{dC(t)}{dt} = 0 \tag{A3}$$

Carbon sequestration rate, $\frac{dC(t)}{dt} \geq 0$ and its derivative, $\frac{d^2C(t)}{dt^2} \leq 0$. Also, the carbon sequestration rate is proportional to the extent to which the soil is depleted of the carbon content. Therefore,

$$\frac{dC(t)}{dt} \propto (C^* - C(t)) \tag{A4}$$

Equation (A4) is solved assuming the proportionality constant to be s, giving us:

$$C^* - C(t) = ke^{-st} \tag{A5}$$

Using the condition (A2), one gets:

$$C(t) = C^* - (C^* - \tilde{C})e^{-st} \tag{A6}$$

A.1.2 Carbon release

The analogous conditions for carbon release dynamics are the following:

$$\lim_{t\to\infty} C(t) = C_o \tag{A7}$$

$$\lim_{t\to 0} C(t) = \tilde{C} \tag{A8}$$

Carbon content asymptotically approaches C_o as $t \to \infty$. Hence,

$$\lim_{t\to\infty} \frac{dC(t)}{dt} = 0 \tag{A9}$$

Carbon release rate, $\frac{dC(t)}{dt} \leq 0$ and its derivative, $\frac{d^2C(t)}{dt^2} \geq 0$. The carbon release rate is proportional to the carbon content of the soil. Therefore,

$$\frac{dC(t)}{dt} \propto -(C(t) - C_o) \tag{A10}$$

Assuming the proportionality constant equal to *s'*, one gets:

$$C(t) = C_o + (\tilde{C} - C_o)e^{-s't} \tag{A11}$$

Alternately, the carbon release dynamics can be thought of as an inverse process of carbon sequestration with C^* replaced by C_o and s replaced by s' in the equation (A6).

A.2 Environmental Policy Integrated Climate (EPIC) simulation results

Figure A.1 shows the distributions of SOC and yield obtained with CT for corn in fields belonging to different hydrologic groups. These SOC distributions represent stable SOC levels after the fields have been tilled with CT for an extended period. Hydrologic group

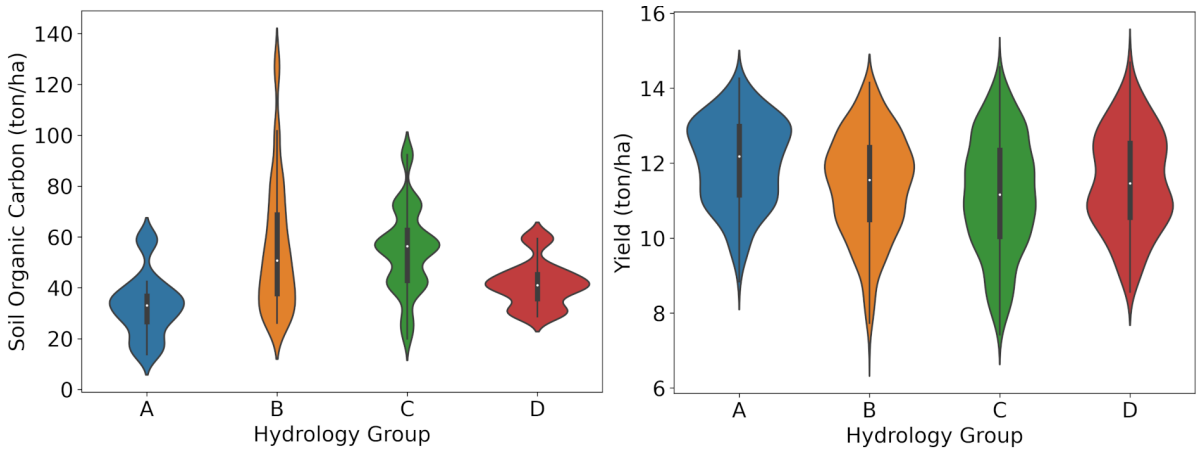


Figure A.1: Distributions of SOC levels (left) and corn yield (right) across different fields under conventional tillage from EPIC simulations. Hydrologic group B exhibits the highest SOC and the lowest yields. Hydrologic group D has the lowest SOC levels but displays a bimodal distribution. Yields in hydrologic group D are relatively high and show significant variability. SOC levels in hydrologic group A also exhibit a bimodal distribution.

A has the smallest average SOC, whereas group C has the largest average SOC. Hydrologic group B shows the greatest range of stable SOC values. The corn yield distributions for CT is relatively constant across the different hydrologic groups, although the average yield is slightly higher for the fields in hydrologic group A.

Appendix Figure A.3 shows distributions of SOC gains and yield losses for the no till (NT) and reduced till (RT) practices for the fields belonging to different hydrologic groups. It is observed that the yield loss is smallest in hydrologic group A when either no-till (NT) or reduced till (RT) is employed, but it is also associated with smallest SOC gain. Hydrologic group B shows largest average SOC gain but also the largest yield loss.

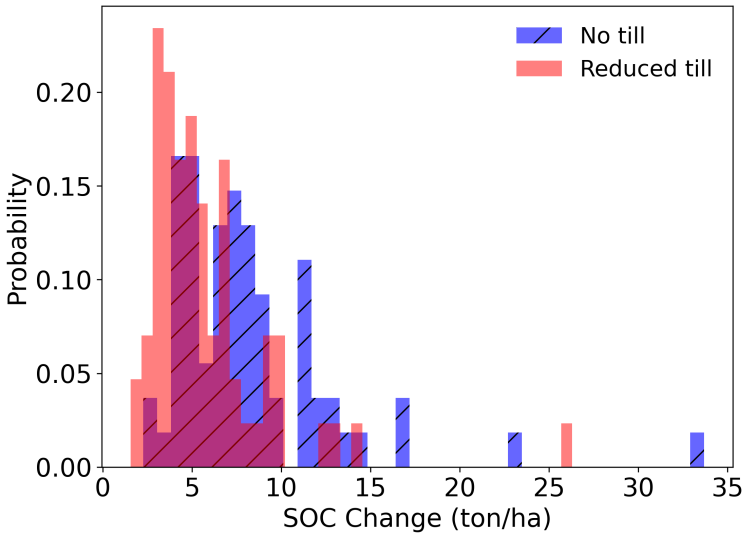


Figure A.2: Distribution of increase in SOC under no till and reduced till practices for corn cultivation from EPIC simulations. The shaded blue histograms represent no till, while the pink histograms represent reduced till. Purple regions indicate overlapping areas between the no-till and reduced-till histograms. Overall, greater SOC increase is observed under no till compared to reduced till.

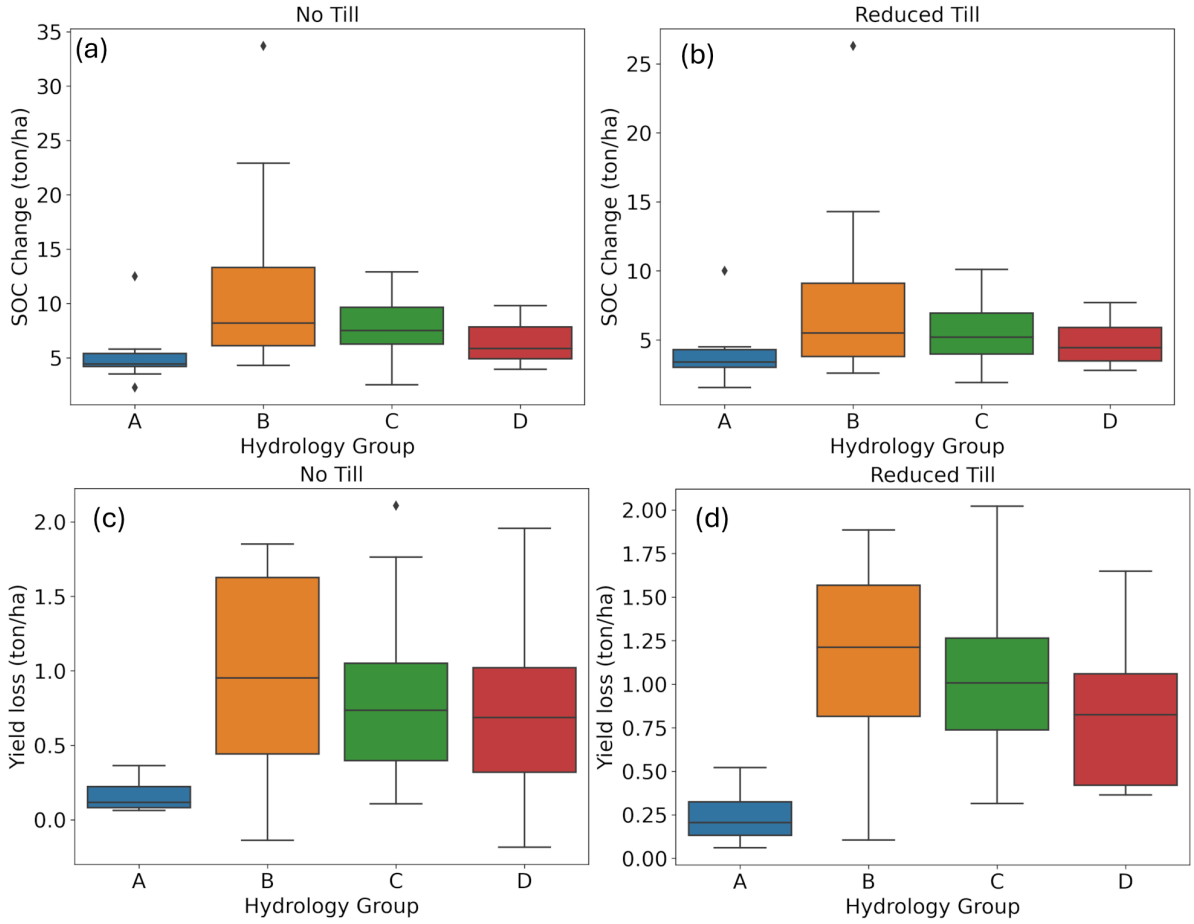


Figure A.3: Distribution of increase in SOC for fields in different hydrologic groups under (a) no-till and (b) reduced till practices from EPIC simulations. Hydrologic group A exhibits the smallest SOC increase and the smallest yield loss. Hydrologic group B shows the largest SOC increase as well as the largest yield loss.

Table 5: Dataset summary by hydrology group.

MUKEY	CSB	HUC	Hyd.	Y_{CT}	Y_{NT}	Y_{RT}	ΔY_{NT}	ΔY_{RT}	s_{NT}	s_{RT}	C^*_{RT}	C^*_{NT}	C_0
168992	618	LowerMaumee	A	10.85	10.78	10.33	0.07	0.52	0.087	0.081	31.92	33.33	24.30
186359	801	Maple	A	12.59	12.22	12.27	0.36	0.32	0.061	0.072	36.30	37.40	23.40
187044	268	Maple	A	12.11	12.01	11.98	0.10	0.13	0.041	0.047	51.20	53.70	41.40
199256	145	Macoupin	A	12.40	12.14	11.95	0.25	0.45	0.076	0.066	61.41	62.22	51.70
423949	478	UpperFox	A	13.18	12.96	12.98	0.22	0.20	0.080	0.089	40.20	41.50	29.70
426074	479	UpperFox	A	12.61	12.53	12.54	0.08	0.08	0.091	0.091	29.49	30.40	22.60
426400	350	Sugar	A	12.56	12.49	12.49	0.06	0.06	0.078	0.080	39.40	40.50	29.70
2399566	118	LowerMaumee	A	10.67	10.55	10.34	0.12	0.33	0.089	0.089	15.35	16.06	12.60
2861390	509	UpperFox	A	11.38	11.18	11.22	0.20	0.16	0.074	0.089	21.50	22.50	17.00
162995	676	Sugar	B	11.37	10.42	10.16	0.95	1.21	0.024	0.033	139.60	148.20	103.30
163013	344	Sugar	B	11.20	10.18	9.90	1.02	1.31	0.070	0.081	34.50	36.80	22.20
163021	492	Sugar	B	9.36	8.75	8.32	0.61	1.04	0.068	0.063	75.35	77.57	62.30
163067	914	Sugar	B	13.10	11.25	11.35	1.85	1.74	0.026	0.030	125.40	132.80	78.50
168216	291	LowerMaumee	B	11.92	11.75	11.45	0.17	0.47	0.063	0.067	61.00	62.60	46.70
169019	715	LowerMaumee	B	10.14	9.61	9.09	0.53	1.05	0.036	0.045	90.10	95.40	74.50
182564	811	UpperFox	B	12.02	11.43	11.08	0.59	0.94	0.068	0.074	49.90	52.20	34.50
182578	620	UpperFox	B	10.06	10.20	9.70	-0.14	0.37	0.074	0.075	30.81	32.50	22.30
182692	281	UpperFox	B	12.21	11.06	10.90	1.14	1.31	0.046	0.060	70.60	74.90	56.10
186396	387	Maple	B	11.23	9.55	9.54	1.68	1.69	0.051	0.067	45.40	47.80	30.60
186396	898	Maple	B	11.23	9.57	9.55	1.67	1.68	0.051	0.067	45.40	47.80	30.60
199218	979	Macoupin	B	11.13	10.91	10.31	0.22	0.81	0.069	0.069	71.00	73.90	55.50
211741	537	Macoupin	B	11.57	11.12	10.82	0.44	0.74	0.032	0.039	91.30	95.50	63.20
211786	76	Macoupin	B	11.11	10.83	10.45	0.28	0.65	0.086	0.084	29.90	31.00	20.50
422801	667	UpperFox	B	13.17	11.39	11.60	1.78	1.57	0.048	0.056	62.50	66.50	34.10

Continued on next page

Table 5 – *continued*

MUKEY	CSB	HUC	Hyd.	Y_{CT}	Y_{NT}	Y_{RT}	ΔY_{NT}	ΔY_{RT}	s_{NT}	s_{RT}	C^*_{RT}	C^*_{NT}	C_0
423956	972	UpperFox	B	11.78	11.69	11.68	0.09	0.11	0.080	0.089	29.70	30.60	23.90
425297	111	Sugar	B	10.09	8.46	8.20	1.63	1.89	0.078	0.085	45.15	47.90	32.40
425303	630	Sugar	B	12.80	11.51	11.54	1.29	1.25	0.057	0.066	45.90	48.40	25.70
425493	598	UpperFox	B	13.17	11.41	11.60	1.76	1.57	0.048	0.053	62.90	66.50	34.10
426340	800	Sugar	B	9.85	9.04	8.75	0.80	1.10	0.071	0.053	57.97	59.69	47.20
678770	647	Sugar	B	11.20	10.18	9.90	1.02	1.31	0.070	0.081	34.50	36.80	22.20
169097	421	LowerMaumee	C	10.14	9.90	9.59	0.24	0.56	0.052	0.060	58.48	60.10	43.60
169107	433	LowerMaumee	C	13.04	12.63	12.51	0.41	0.53	0.070	0.066	56.16	57.30	40.00
169108	870	LowerMaumee	C	10.87	10.76	10.56	0.11	0.31	0.074	0.067	21.92	22.52	16.60
186399	122	Maple	C	10.61	8.50	8.59	2.11	2.02	0.049	0.071	63.00	66.90	40.30
186399	541	Maple	C	10.61	8.50	8.59	2.11	2.02	0.049	0.071	63.00	66.90	40.30
187290	374	Maple	C	12.98	12.65	12.61	0.33	0.37	0.053	0.062	59.50	61.10	37.30
187302	99	Maple	C	12.84	12.48	12.47	0.36	0.36	0.065	0.078	41.70	42.90	27.80
187833	643	Maple	C	11.30	9.95	9.98	1.35	1.32	0.052	0.070	63.93	66.10	45.50
187859	468	Maple	C	12.00	11.63	11.67	0.37	0.33	0.074	0.087	28.50	29.50	19.00
199167	545	Macoupin	C	9.28	8.93	8.37	0.35	0.91	0.077	0.077	46.46	48.90	35.40
199212	25	Macoupin	C	9.52	8.77	8.33	0.74	1.18	0.060	0.080	77.27	81.40	61.00
199219	678	Macoupin	C	11.99	11.47	11.20	0.52	0.79	0.059	0.069	67.40	69.80	45.30
199224	73	Macoupin	C	10.21	9.82	9.37	0.39	0.85	0.056	0.081	41.71	44.80	28.90
199238	243	Macoupin	C	11.93	11.59	11.28	0.34	0.65	0.059	0.068	61.50	63.80	41.70
199239	55	Macoupin	C	9.66	8.74	8.37	0.92	1.29	0.058	0.078	62.20	66.10	55.80
425271	338	Sugar	C	12.33	11.25	11.11	1.08	1.23	0.048	0.050	63.40	66.20	39.10
425321	888	Sugar	C	12.83	11.81	11.82	1.02	1.01	0.047	0.054	65.80	68.10	39.20
425384	561	Sugar	C	13.04	11.87	11.93	1.17	1.10	0.057	0.063	52.00	54.30	30.30
425391	372	Sugar	C	13.02	12.07	12.04	0.95	0.98	0.059	0.064	49.10	51.00	29.90
425901	508	UpperFox	C	11.31	10.07	10.05	1.24	1.26	0.055	0.064	45.20	47.20	29.90

Continued on next page

Table 5 – *continued*

MUKEY	CSB	HUC	Hyd.	Y_{CT}	Y_{NT}	Y_{RT}	ΔY_{NT}	ΔY_{RT}	s_{NT}	s_{RT}	C^*_{RT}	C^*_{NT}	C_0
426067	779	UpperFox	C	13.10	12.43	12.41	0.67	0.69	0.058	0.064	50.90	52.70	31.50
728449	314	Macoupin	C	11.31	10.50	10.22	0.81	1.09	0.052	0.072	58.80	62.00	38.00
1536637	145	LowerMaumee	C	9.71	9.31	8.88	0.40	0.84	0.058	0.056	76.15	78.40	62.90
1536637	800	LowerMaumee	C	9.71	9.31	8.87	0.40	0.84	0.058	0.056	76.15	78.40	62.90
1536637	848	LowerMaumee	C	9.71	9.30	8.87	0.41	0.84	0.056	0.056	76.15	78.50	62.90
1536661	690	LowerMaumee	C	9.88	9.15	8.78	0.73	1.11	0.041	0.051	98.20	102.40	78.00
1539735	155	LowerMaumee	C	9.88	9.15	8.78	0.73	1.11	0.041	0.051	98.20	102.40	78.00
1721557	436	Macoupin	C	9.66	8.74	8.37	0.92	1.29	0.058	0.078	62.20	66.10	55.80
2998376	559	Maple	C	10.51	9.53	9.24	0.99	1.27	0.060	0.062	75.25	77.30	58.90
3117240	503	Maple	C	10.93	9.27	9.23	1.66	1.71	0.055	0.072	33.20	35.30	21.60
3117289	658	Maple	C	11.85	10.09	10.12	1.76	1.73	0.055	0.067	48.90	50.90	30.90
169002	77	LowerMaumee	D	12.02	11.96	11.65	0.05	0.36	0.060	0.065	39.59	40.80	27.20
169123	738	LowerMaumee	D	10.17	10.36	9.78	-0.18	0.40	0.067	0.066	43.13	44.24	33.50
186999	698	Maple	D	13.12	12.71	12.69	0.41	0.43	0.051	0.058	65.30	66.80	43.40
187314	767	Maple	D	10.80	8.84	9.15	1.96	1.65	0.065	0.082	35.30	36.10	22.30
199209	574	Macoupin	D	11.79	11.36	11.09	0.43	0.70	0.065	0.071	47.80	49.90	29.30
425850	736	UpperFox	D	12.92	11.76	11.83	1.15	1.09	0.056	0.063	48.10	50.20	29.20
753459	871	Sugar	D	10.98	10.04	10.03	0.94	0.95	0.050	0.063	50.40	52.40	34.70
1591203	15	Sugar	D	10.21	9.24	9.16	0.98	1.05	0.065	0.074	32.40	33.90	21.30